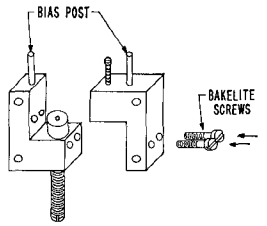

Fig. 1. Split guide mount featuring cold finger.

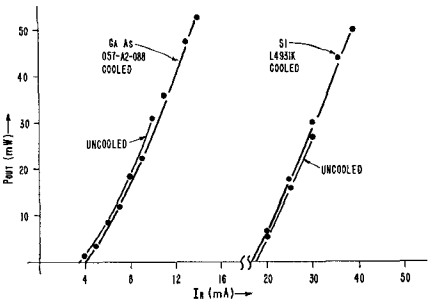

Fig. 2. Variation of RF output power with bias current for both cooled and uncooled operation.

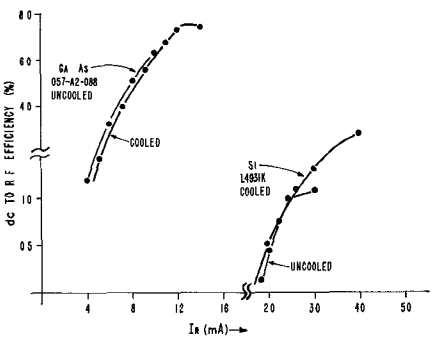

Fig. 3. Oscillator efficiency as a function of reverse-bias current for cooled and uncooled operation.

of cooling resulted in a 14 dB increase in gain at this point. The bandwidth was measured at the 0 dBm input level and was found to be 69 MHz.

Reflection amplifier noise figure measurements were also made under high-gain conditions (10 to 30 dB). Fig. 5 shows the dependence of the noise figure on avalanche current as measured in identical circuits for a Si and GaAs varactor diode having identical avalanche frequencies and the same magnitude of negative conductance. The GaAs reverse current was varied from 6 to 14 mA, and the corresponding noise figure varied from 32 to 25.5 dB. The Si amplifier had a 61 dB noise figure at 10 mA and 38 dB at 30 mA. Between 10 and 12.5 mA of reverse current, the Si device was near the threshold of amplification, giving an excessively high-noise figure. In general, the GaAs device is 13.0 dB less noisy than the equivalent Si device.

Significant improvement in the operation of avalanche transit time amplifiers and oscillators is obtainable by cooling.[6] At room temperature the effects of excessive junction heating limits the performance of these devices. Cooling has the effect of extending the

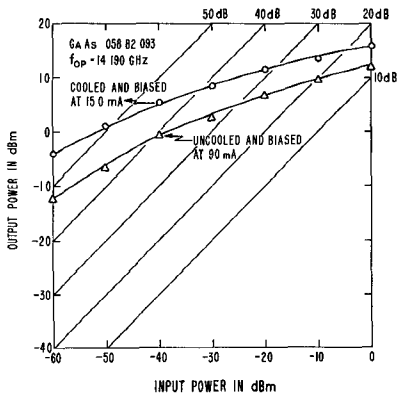

Fig. 4. Gain as a function of input power for GaAs avalanche amplifier.

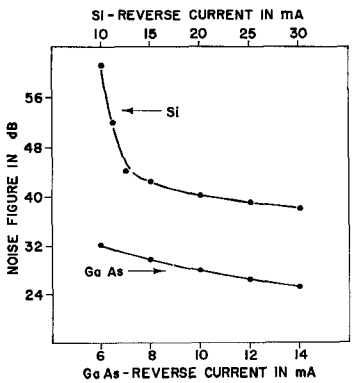

Fig. 5. High-gain noise figure as a function of reverse current.

operating range of these devices which resulted in improved oscillator output efficiencies, and improved amplifier gain and noise figure. The need for good thermal heat sinking and good thermal resistance of junctions seems to be apparent. Then, with these improvements, optimum operation comparable to the cooled results should be derived from uncooled devices.

JOSEPH J. BARANOWSKI
VINCENT J. HIGGINS
FRANK A. BRAND
Electronic Components Lab.
USAECOM
Ft. Monmouth, N. J.

REFERENCES

[1] F. A. Brand, V. J. Higgins, J. J. Baranowski, and M. A. Druesne, "Microwave generation from avalanching varactor diodes," *Proc. IEEE (Correspondence)*, vol. 53, pp. 1276–1277, September 1965.

[2] V. J. Higgins, F. A. Brand, and J. J. Baranowski, "Characteristics of varactor diodes biased into avalanche," presented at the Internat'l Electron Devices Meeting, Washington, D. C., October 20, 1965.

[3] ——, "Performance characteristics of CW silicon and GaAs avalanche diode oscillators," presented at the Internat'l Microwave Symp., Palo Alto, Calif., May 1966.

[4] J. J. Baranowski, V. J. Higgins, and M. J. McCormick, "Avalanche transit time diodes," *Microwaves*, vol. 5, pp. 24–31, August 1966.

[5] M. J. McCormick, V. J. Higgins, and J. J. Baranowski (to be published).

[6] C. B. Swan, "The importance of providing a good heat sink for avalanching transit time oscillator diodes," *Proc. IEEE (Letters)*, vol. 55, pp. 451–452, March 1967.

Broadband Fixed-Tuned Acoustic Delay Lines

This correspondence is concerned with the design of broadband fixed-tuned delay lines to operate at *L*- and *S*-band frequencies. These delay lines utilize layer transducers incorporating CdS thin films of the type used by deKlerk,[1] sapphire delay media, and suitable electrical matching networks in either coaxial or in strip transmission line.

The impedance seen by an electrical network terminated in the transducer shown in Fig. 1(a) has been obtained in the past[2]–[6] by solving the piezoelectric equations subject to the indicated boundary conditions. The impedance in Evans' notation neglecting dielectric losses in the transducer is

$$Z = \frac{-jL}{\omega A\epsilon} + \frac{k^2V}{\omega^2 A\epsilon} \cdot \left[\frac{\frac{2\xi_0}{-\xi_2}\left(1 - \frac{1}{\cos\beta L}\right) + j\tan\beta L}{1 + j\frac{\xi_0}{\xi_2}\tan\beta L}\right]$$

which may be written, by breaking into real and imaginary parts, as

$$Z = R(\omega) - jX_c - jX(\omega)$$

where the real part of the impedance $R(\omega)$ may be termed the acoustic radiation resistance, X_c is the normal capacitive reactance, and $X(\omega)$ is a small additional reactance. For many transducer configurations using CdS in the gigahertz range, $R(\omega)$ may be as small as 0.01 ohm making possible only loose coupling from electromagnetic to acoustic energy. Correspondingly large mismatches are obtained. This situation may be altered by adjusting the ratio ξ_0/ξ_2. Since ξ_2 is the acoustic impedance seen looking into the right electrode of Fig. 1(a), suitable metallic layers may be used to adjust the value of ξ_2. Fig. 1(b) is a plot of values of $R(\omega)$ and $X(\omega)$ versus normalized frequency for several values of ξ_0/ξ_2. Here a normalizing factor $(\pi/4k^2)(f/f_0X_c)$ has been used to allow for general transducer materials. The relationships of Fig. 1(b) are useful in bandwidth considerations indicating that a device having a large $R(\omega)$ yields a narrowband device. For cases in which ξ_2 is obtained from multilayer electrode arrangements, the ratio ξ_0/ξ_2 will exhibit a frequency dependence and the relationships will be modified.

In order to design broadband delay devices at *L*- and *S*-band frequencies, a computer program was prepared in which either a two- or three-step Chebyshev electrical transformer is terminated by the acoustic transducer of Fig. 1(a). A VSWR ripple of 1.70 to 1 was selected when the network is terminated by the real part of the impedance $R(\omega)$, and provision was made in programming where the impedance ξ_2 would represent a general impedance formed by the acoustic delay media and suitable metallic or dielectric layers.

Multilayer electrode configurations have

Manuscript received June 17, 1967; revised August 8, 1967. The work reported here was supported in part by the Harry Diamond Labs., Washington, D. C. under Contract DAA 39-67-C-2042.

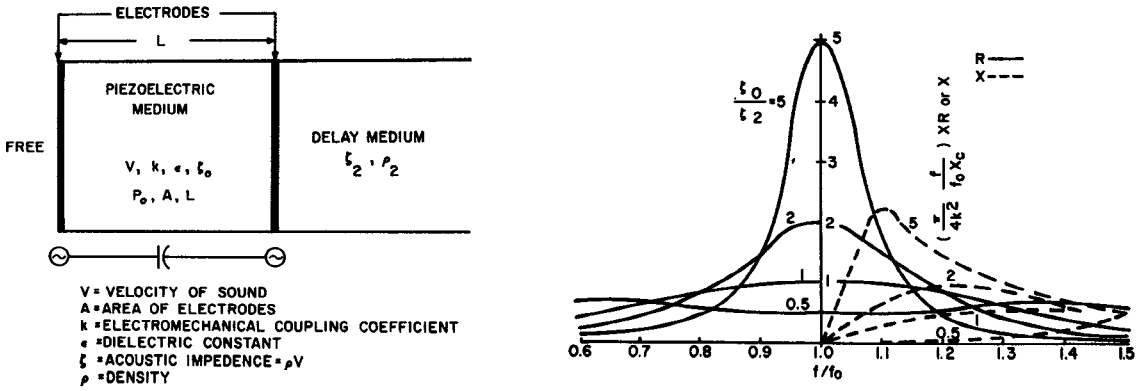

Fig. 1. Transducer configuration and calculated response for various acoustic loads.

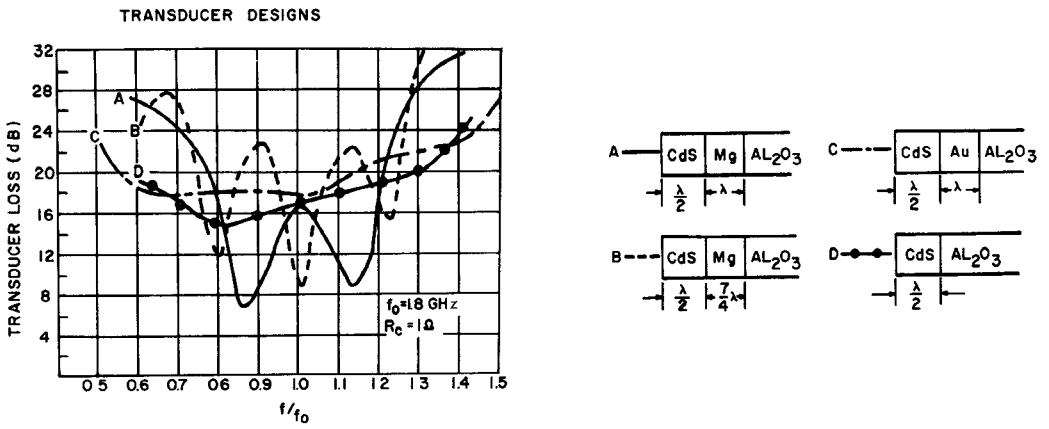

Fig. 2. Theoretical transducer designs and frequency responses.

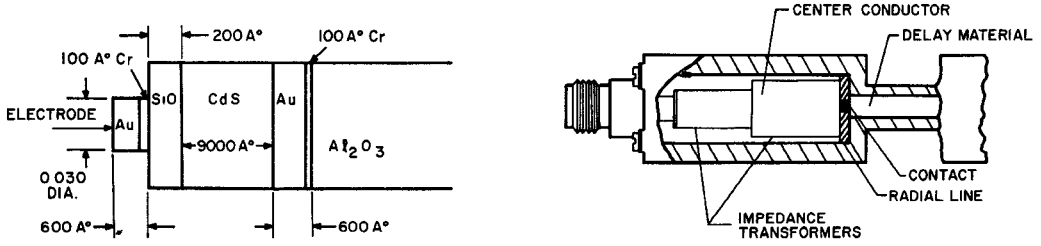

Fig. 3. Transducer implementation and coaxial matching transformers. (a) Transducer design. (b) Coaxial delay device.

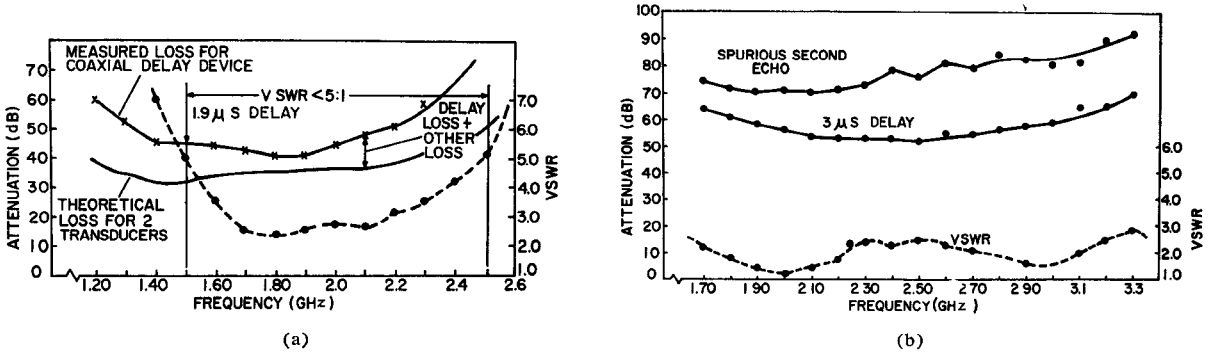

Fig. 4. Experimental delay line data.

been investigated as shown in Fig. 2. In calculating these curves, a 50 ohm source impedance has been assumed while an additional series contact resistance of value 1 ohm has been included. This contact resistance has been measured in physical configurations where springlike contacts are used in connecting the RF circuit to the acoustic transducer electrode. In these characteristics, metallic acoustic transformers have been used which present $n\lambda/4$ ($n=1, 3, 5, 7, \cdots$) matching conditions as the frequency is swept over the band of interest. For example, in Design A of Fig. 2 a thickness of magnesium is used which results in $3\lambda/4$ and $5\lambda/4$, matching at frequencies above and below the center frequency.

The original thought in using the $n\lambda/4$ metallic transformers was that frequency stagger tuning between input and output transducer might be used to advantage. After evaluating the various transducer configurations, Design D was chosen as representing the best electrical characteristics while offering ease of implementation. For example, Designs A and B exhibit steep attenuation skirts at the band edges, largely negating the advantages of stagger tuning. Moreover, should stagger tuning be used here, stringent tolerances on CdS thicknesses would be required.

In the design of 1.8 GHz delay devices, a physical transducer patterned after Design D of Fig. 2 has been used. This design is shown in Fig. 3(a). Thin combined layers of chromium and gold are used as electrodes while a 200 Å layer of SiO is included to insure isolation between the electrodes should pin holes be present in the CdS films. The CdS thickness is reduced from 12 400 to 9000 Å to compensate for resonator loading by the additional films. The attenuation characteristics for the overall transducers have been calculated and are virtually the same as in the original design. The diameters of the transducers are 0.030 inch to provide for the largest possible $R(\omega)$ without adding significant diffraction losses when used in delay devices.

Two classes of 1.9 μs delay lines have been designed and fabricated using the transducers of Fig. 3(a). In the first type, the coaxial matching structure of Fig. 3(b) has been used. Here, a two-section Chebyshev transformer having impedances of 15.4 and 2.7 ohms is used for matching. The 2.7 ohm section is partially in coax and partially in a radial transmission line which, in turn, is terminated by the acoustic transducers. The experimental attenuation and VSWR data for this device are given in Fig. 4(a). The theoretical loss for the two transducers also is included, and it is seen that the difference between the two curves can be accounted for by loss in the delay media, mismatch loss at the band edges by diffraction loss in the media, and in possible misalignment of the two transducers. By slightly redesigning the coaxial transformers and incorporating a small absorber in the coaxial section of the device, the VSWR has been reduced to below 2 to 1 over the frequency band from 1.35 to 2.3 GHz.

The second type has been designed in strip transmission line to utilize the same acoustic transformers. In this configuration, a three-section Chebyshev matching transformer is utilized exhibiting impedances of approximately 24, 7, and 2 ohms. In these matching sections, 0.030 and 0.010 inch ground plane spacings are used. The attenuation data for this device are approximately the same as for coaxial design while an improvement in VSWR is obtained (VSWR is less than 2 to 1 across a 50 percent band).

Another delay line has been designed to operate at a center frequency of 2.5 GHz. In this design, strip transmission-line matching has been used, and the individual acoustic transducers have been stagger tuned to center frequencies of 2.4 and 2.6 GHz, respectively. Experimental data for this device are given in Fig. 4(b). It is seen that a 53 dB insertion loss ± 1 dB is obtained from 2 to 3 GHz with a 60 dB bandwidth ranging from 1.8 to 3.2 GHz.

Other broadband and narrowband fixed tuned delay devices have been designed to operate at center frequencies as low as 450 MHz through UHF and L bands. In all cases, theory and experiment are in good agreement. Overall insertion losses as low as 11 dB have been obtained for 4 μs delay in the 450 MHz unit. The L- and S-band delay devices described in this correspondence have operated for several months without failure and have been subjected to 1 watt peak power levels.

Acknowledgment

The authors are indebted to Dr. J. deKlerk for depositing the CdS film used in these experiments and to H. W. Cooper and D. O'Sullivan for their overall contributions to this program.

L. R. Whicker
P. F. Carcia
G. E. Evans
Microwave Physics Group
Westinghouse Electric Corp.
Baltimore, Md. 21203

References

[1] J. deKlerk and E. F. Kelly, "Coherent phonon generation in the gigacycle range via insulating cadmium sulfide films," *Appl. Phys. Lett.*, vol. 5, p. 2, July 1964.
[2] W. H. Haydl, K. Blotekjar, and C. F. Quate, *J. Acous . Soc. Am.*, vol. 36, p. 1670, 1964.
[3] D. K. Winslow and H. J. Shaw, "Multiple film microwave acoustic transducers," *IEEE Internat'l Conv. Rec.*, pt. 5, pp. 26–31, 1966.
[4] W. Crofut, "Broadband microwave acoustic delay lines," *Microwave J.*, pp. 65–72, January 1966.
[5] G. E. Evans, "Piezoelectric transducers for microwave ultrasonics," Ph.D. dissertation, University of Maryland, College Park, 1967. Also, G. E. Evans, "Fixed tuned CdS transducer," presented at the Ultrasonics Symp., 1966.
[6] D. J. Page, "Cadmium sulfide thin film devices," Westinghouse Electric Corp., Baltimore, Md., Sci. Paper 66-1F10-FILMD-P5, April 1966.